# A Robust Edge Detection Method for Gated Radionuclide Ventriculograms

A. Dennis Nelson, Gary J. Muswick, Raymond F. Muzic, Jr. and Xavier Descamps

*Division of Nuclear Medicine, Department of Radiology, University Hospitals of Cleveland, Case Western Reserve University, School of Medicine, Cleveland; and Trionix Research Laboratory, Twinsburg, Ohio*

We present a myocardial edge detection technique that was developed for fast, reproducible measurements of left ventricular ejection fraction in the clinical setting. **Methods:** This myocardial edge detection method compares three edge parameters—count amplitude and first and second count derivatives—in three consecutive locations along a radius to a predetermined template of these values. Each of the radii, defined at 10-degree intervals, has different template values that permit accurate edge detection even though adjacent structures, such as the left atrium and the right ventricle, alter edge parameters. The template for edge detection is based on either the average edge parameters determined from manually defined edges in 15 patients (automatic method) or an operator-defined edge in the first frame (semiautomatic method). **Results:** The edge detection methods were tested in 100 patients, and intraobserver and interobserver variabilities as well as comparison with clinically obtained ejection fractions were calculated. The standard error of the estimate was less than 3.1% for all observer comparisons. In 15 patients with both high-count (400,000 counts per image) and low-count (50,000 counts per image) studies, the mean absolute difference in ejection fraction was 2.6% for intraobserver comparisons. **Conclusion:** A robust myocardial edge detection technique was developed that is applicable for routine clinical use.

**Key Words:** gated blood-pool scintigraphy; left ventricular ejection fraction; reproducibility

**J Nucl Med 1996; 37:685–689**

$\mathbf{G}$ated equilibrium radionuclide ventriculography with the radioactive tracer $^{99m}$Tc is a routine procedure for determining left ventricular ejection fraction (1–5). Manually defined regions of interest for determination of ejection fraction have been shown to have large interobserver variability, whereas automated techniques have been shown to reduce this variability (3). Automated edge detection techniques are typically based on one or more of three parameters: (a) image count amplitude; (b) first count derivative and (c) second count derivative (6,7). The constant amplitude threshold method is unreliable because adjacent structures, such as the left atrium, aortic outflow tract and right ventricle, affect count levels to varying degrees at the left ventricular border. Similarly, the first and second count derivatives are also affected by adjacent structures, so that uniform threshold methods result in edge detection that is inconsistent for different ventricular regions. An additional problem for count-derivative determinations is their inherent sensitivity to noise.

Methods based on the maximum of the first derivative or zero crossing of the second derivative tend to underestimate the size of the ventricular border (8). The ventricular counts are reduced for these methods because left ventricular counts exist outside the defined edges due to scatter and finite instrument resolution.

Techniques based on the maximum of the second derivative tend to have edges that are too large (8).

In this article, we present an edge detection method for ejection fraction calculation that is based on edge parameter values that vary as a function of anatomic location. The method is clinically efficacious because: (a) computation time is short, (b) interobserver and intraobserver variabilities are low and (c) the method yields consistent results for high- and low-count studies.

## METHODS

### Edge Detection

The left ventricular edge detection method is based on a radial coordinate system with 36 radii and the origin at the centroid, based on area, of the left ventricular region. The radii are 1 pixel wide and extend from the centroid of the left ventricle to the edge of the image. Zero degrees is defined as a horizontal radius that extends from the centroid through the lateral wall. At 1-pixel-wide intervals from the centroid to the edge of the image, the edge parameters of count amplitude and first and second count derivatives are calculated along each of the radii. The method used for derivative calculations is described in a later section (see Derivative Calculations). All images are interpolated from original size to a 128 × 128 matrix before analysis, and distances are defined according to these 128 × 128-pixel sizes. Images are spatially smoothed with a Metz filter (9,10) and temporally smoothed with a 1-2-1 filter.

The template of edge parameter values used for edge detection is unique for each radius and has values based on the analysis method—automatic or semiautomatic. The derivation of these edge parameter values is described in the following two sections. The template values used for edge detection along each radius are defined at the ventricular edge and 1 pixel on either side. To test each point along the radius as a potential edge location, the edge parameters calculated for that point and the two adjacent radial locations are compared with the desired template values. The sum of the square differences between measured edge parameters and template values is calculated for each three-point series of locations along the radius. The center point of the three-point series with the smallest square difference compared with template values was selected as the edge for each radius.

*Semiautomatic Method.* In the semiautomatic method, the operator draws the left ventricular outline in the first image frame. This outline is used to generate a template of edge detection parameters that are used to detect the ventricular edge in subsequent frames. The centroid of this outline is calculated, and the intersection of 36 equally spaced radii with the outline is determined. The template for edge detection in the following frames is made by calculating all three edge parameters for each radius at three adjacent radial locations centered at the ventricular edge. For each image, the maximum count level and maximum first and second count derivatives are determined for all radial locations in that image. These maximum values are used to express all edge detection parameters in percent of their maximum value for that image.
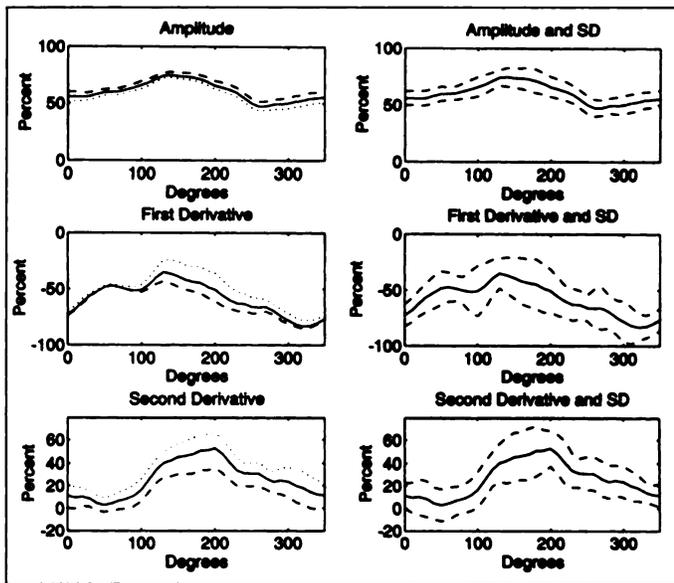
**FIGURE 1.** Left panels show the average value of count amplitude and first and second derivatives for three adjacent pixels centered on the ventricular edge in 15 patients. The value at the ventricular edge (—), the pixel inside the edge (---) and the pixel outside the edge (····) are shown. Zero degrees represents a radius from the centroid through the lateral wall. The radii proceed counterclockwise so that the septum is at 180°, and the apex is at 270°. Right panels show the mean value at the ventricular edge (—) and the mean value ± s.d. (---) of edge parameter values.

In each image frame after the first frame, the centroid is initially assumed to be at the same location as the previous frame. The edge is determined as the midpoint of the three-point radial series, which minimizes the mean square difference between the operator-defined template and measured edge parameters for each radius. This ventricular edge is constrained to be within an operator-determined distance from the edge in the previous frame, which represents the maximum expected movement due to wall motion. If the distance of the centroid based on the detected edge outline is greater than 3.0 pixels from the initially assumed centroid, the location of the centroid is updated, and the edge is determined iteratively until the difference in centroid locations between successive iterations is less than 3.0 pixels. The final edge is the result of a spatial filter of this edge. The distance from the centroid to each edge point is calculated, and the final edge points are calculated on the basis of a 1-2-9-2-1 distance smoothing filter.

*Automatic Method.* Whereas the template for edge detection is unique for each patient with the semiautomatic method, the template for the automatic method is the same for all patients. The template for the automatic method was calculated as the average of 15 templates previously generated with the semiautomatic method. The patient templates used for automatic template generation represented a consecutive series of patient studies, none of whom were included in any other studies. The ventricles were aligned for these 15 patients on the basis of apical location before inclusion in the template. To determine apical location, the distance from the centroid to the myocardial edge was determined for all radii between 180° and 360°. These radii extend from the septum to the apex and then to the lateral wall. The radius with the longest length was defined as the apex, and the edge parameters for this radial location were translated to be at 270° before inclusion in the template. The template represents the average normalized values from all 15 patients (Fig. 1).

Edge detection with the automatic analysis method requires the operator to define an initial estimate of the center of the left ventricle in the first frame. Potential edge locations for the first frame are determined from this center to the maximum inscribed circle possible in the image frame. The ventricular border at each radial location is determined that results in the smallest minimum square error compared with template values for that radius. An example of a typical patient profile and template values at the detected edge location is shown in Figure 2.

The initially defined edge in the first frame requires refinement that is not required in succeeding frames. Occasionally, an edge of the aorta or right ventricular lateral wall is incorrectly identified as the left ventricular border for the first frame. These outliers are detected as having a distance from the preceding edge location that is greater than one-half times the median distance of all edge points from the center. These outlier points are temporarily assigned edge locations equal to the radial distance of the preceding point to create a smooth edge. A new myocardial edge is then defined that is constrained to be within an operator-defined distance, representing maximum movement due to wall motion, from this smooth edge. This myocardial edge is also determined based on minimizing the mean square error differences with the template. The centroid of this edge is determined and used as a new center of the radial coordinate system.

The next edge refinement in the first frame allows for apical alignment between the template and patient image. The ventricular edge is determined such that it has the minimum square error compared with the template for rotations from between 60° clockwise to 60° counterclockwise. In the following frames,
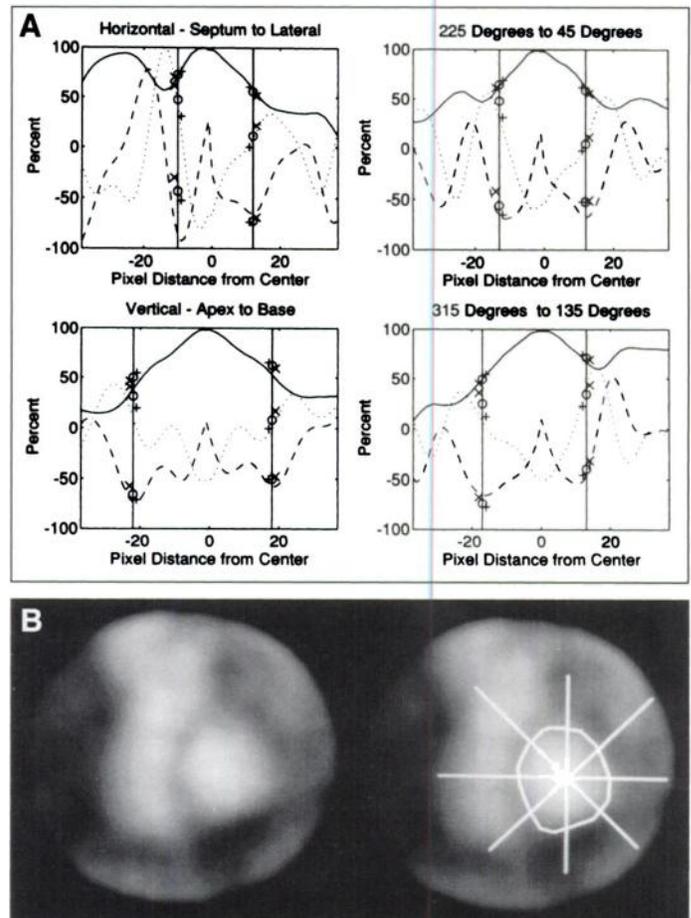


**FIGURE 2.** (A) Count and derivative profiles for four diameters through the ventricle, thus, 8 of the 36 radii actually calculated are shown (B). The template values derived from 15 patient studies are for 1 pixel inside the edge (+), 1 pixel at the edge (0) and 1 pixel outside the edge (×). The vertical solid line represents the radial distance detected as the ventricular edge. The solid curve is the amplitude, dashed curve the first derivative and dotted curve the second derivative. The scintigram (B) shows the detected myocardial edge and location of radii included in plots.

template rotation is a maintained constant. The same criteria used with the semiautomatic method to constrain ventricular edge definition, based on ventricular motion and redefinition of the centroid location, were applied for frames after the first frame. The final edge is the result of a spatial filter as defined for the semiautomatic method.

*Derivative Calculations.* The first- and second-count derivative calculations were based on fourth-order polynomial fits to radial count profiles. The width of the radial segment used for polynomial fits was under operator control and was typically 17 pixels. The first and second count derivatives were calculated from the fitted polynomial for the center pixel of the segment. To evaluate derivatives for adjacent radial locations, the entire segment was shifted 1 pixel, and a new polynomial fit was performed.

*Edge Detection Variables.* The operator selects three variables that affect edge detection. Maximum motion is the parameter that sets the radial search limit to search for the ventricular edge from the previous ventricular edge. This parameter also sets the search limit from the smoothed edge in the first frame of the automatic method. The derivative width parameter sets the radial length, which is used to determine the fourth-order polynomial fit at each radial location and thus the first- and second-derivative values. A smaller ventricle may require a smaller radial length interval for determination of fits to radial count profiles. A threshold parameter modifies all edge detection template values on the basis of a linear fit in the radial direction for each edge threshold parameter. The effect of a positive threshold value on template parameters would be observed in Figure 1 as a movement of the dashed line toward the solid line and the solid line toward the dotted line. A positive threshold parameter will increase the size of the ventricular border, whereas a negative value will decrease the size of the edge.

## Background Region of Interest

The background region of interest is defined in the frame with the fewest total counts in the left ventricular region of interest. Thirty regions are considered potential background regions of interest. The region with the smallest average counts per pixel was automatically defined as the background region. The inner edge of each possible background region is either 2, 4, 6, 8 or 10 pixels away from the ventricular edge, and the region width is 5 pixels. Six angular locations are included from 240° to 340°, each a width of 40°. The operator is given the option to modify the computer-defined background region.

## Patient Selection

All patients included in this analysis were referred for clinically indicated gated blood-pool studies. The patients represent a consecutive series obtained in four groups. Each patient's red blood cells were labeled using an in vivo procedure with [$^{99m}$Tc]-pertechnetate. The camera was positioned in a left anterior oblique projection to provide maximum separation between the right and left ventricles. Each patient study included an imaging sequence such that at least one 64 × 64 frame had 400,000 total counts. In 15 patients, an additional scan was obtained such that the maximum total counts in a frame was 50,000 counts. Image magnification was altered by a technologist before acquisition to be of adequate size for qualitative wall motion evaluation.

All 100 patients included in the observer variability measurements had typical clinical determination of left ventricular ejection fraction, which included initial edge detection using an MDS A$^3$ computer system (Medasys Acquisition Corp., Norcross, GA). The 15 patients with low-count studies were not included in this group of 100 patients. The 15 patients included for template generation were also not included in the 100 patients studied for variability determination. The MDS edge detection method was based on the second derivative of a radial count profile and was typically set at

20% of the maximum second-derivative value for all radii. All edges were initially reviewed and edited when necessary by a technologist. The background region was determined automatically in the frame with fewest ventricular counts and was modified manually as necessary. The final ejection fraction and edge definition were confirmed by a nuclear medicine physician.

## Data Analysis

The data from all 100 patients processed for observer variability determination were initially analyzed with both automatic and semiautomatic methods by one observer and were analyzed again after a 6-wk interval by the same observer. A second observer analyzed the data from all 100 patients using both the automatic and semiautomatic methods. In all cases, no left ventricular or background regions were manually modified before ejection fraction calculation. Observer 1 changed edge threshold and maximum motion parameters as necessary to obtain ventricular edges. Observer 2 did not change any edge detection parameters. Observer 1 successfully detected ventricular edges with both techniques in all patients. Observer 2 was successful for all semiautomatic studies and 97 of 100 automatic studies. The typical edge detection parameters used exclusively by Observer 2 were: derivative width minus 17 pixels; maximum motion equals ±8 pixels; and edge threshold minus 0%. The frame with the maximum background-corrected left ventricular counts was defined as the end-diastolic frame. The frame with minimum counts was defined as the end-systolic frame. The difference between background-corrected left ventricular end-diastolic and end-systolic counts divided by background-corrected end-diastolic counts was used to calculate ejection fraction.

The 15 patients with both high- and low-count studies were analyzed by Observer 1 with the automatic analysis method. The typical edge detection parameters described before were used for all 15 patients. No region of interest was modified before ejection fraction calculation in these patients.

## Cardiac Phantom

To test the accuracy of the software, the Vanderbilt cardiac phantom (Capintec Inc., Pittsburgh, PA) was used to simulate a beating heart with known ejection fraction. The phantom was used both with and without a static background representing the right heart, aorta and general background tissue. The phantom was rotated at speeds that mimicked both 60- and 120-bpm heart rates. The phantom was configured for an ejection fraction of 50%. The cardiac phantom was evaluated for both automatic and semiautomatic methods.

## RESULTS

Matching of templates to patient profiles to determine myocardial edges is demonstrated in Figure 3 for both a high-count (400,000 counts per image) and low-count study (50,000 counts per image). The amplitude levels represent values before background subtraction, which are also the values used for edge detection. The edge that was determined with the automatic method is shown. The elapsed time between selection of the center of the left ventricle for the automatic method and display of detected edges on the monitor is 12 sec for a 20-frame study using a Trionix (Trionix Research Laboratory, Inc., Twinsburg, OH) Sun Sparcstation 2. The simple regression line of best fit between ejection fraction measures with high- and low-count studies had a slope of 0.995 and an intercept of −0.62%. The mean absolute difference in ejection fractions was 2.6%.

The interobserver and intraobserver variabilities for ejection fraction measurement in 100 patient studies are summarized in Table 1. The Observer 1 versus MDS row represents the comparison of the first dataset reviewed by observer 1 versus
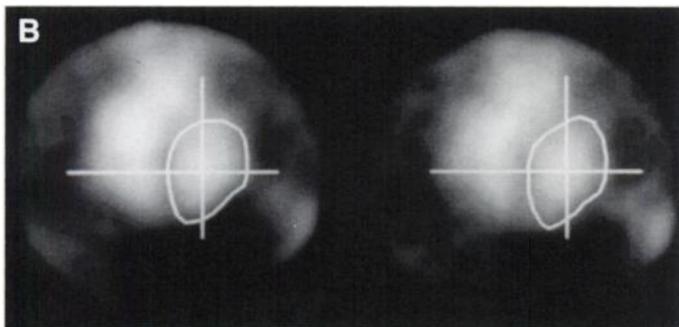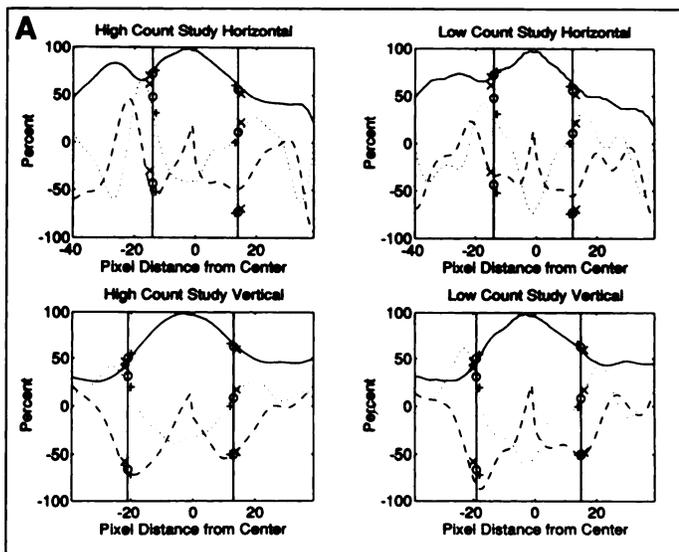
**FIGURE 3.** (A) Count and derivative profiles for vertical and horizontal radii for both a high-count (left panels) and low-count study (right panels). The automatically determined ventricular edges and location of horizontal and vertical radii are shown in the scintigram (B). Format and symbols as in Figure 2.

the clinically determined ejection fractions based on the Medasys $A^3$ computer system.

The automatic technique was not successful in three patients for Observer 2, who did not change edge detection variables. In each case, the automatic technique detected edges outside the left ventricle. Observer 1 modified edge detection parameters with the automatic technique for 8 patients in the first series and 11 in the second series. In all cases, Observer 1 was successful in detecting ventricular edges.

The cardiac phantom studies obtained at rotation speeds equivalent to a heart rate of 60 beats/min, both with added

**TABLE 1**
Ejection Fraction Comparisons

| EF method | Observers | s.e.e. | MAbs | r value | Slope | Int |
|---|---|---|---|---|---|---|
| Semi | Obs 1 vs. Obs 2 | 2.99 | 2.08 | 0.986 | 0.987 | 0.75 |
| | Obs 1 vs. Obs 1 | 1.65 | 1.15 | 0.996 | 0.989 | 0.30 |
| | Obs 1 vs. MDS | 2.99 | 2.74 | 0.985 | 0.973 | −0.46 |
| Auto | Obs 1 vs. Obs 2 | 2.62 | 1.50 | 0.989 | 0.997 | −0.059 |
| | Obs 1 vs. Obs 1 | 1.88 | 1.14 | 0.995 | 0.994 | 0.046 |
| | Obs 1 vs. MDS | 3.01 | 3.16 | 0.985 | 0.968 | −0.892 |

EF = ejection fraction; s.e.e. = standard error of estimate; MAbs = mean absolute difference; r = correlation coefficient; Slope and Int = slope and intercept of simple regression line of best fit, respectively; Semi = semiautomated; Auto = automated; Obs = observer; MDS = Medasys $A^3$ computer system.

background and no background, yielded ejection fractions of 50% for both the automatic and semiautomatic techniques. Similarly, ejection fractions of 48% were obtained for phantom studies obtained at 120 beats/min.

## DISCUSSION

### Validation

The results of the present study demonstrate that consistent ejection fraction measurements can be obtained with this edge detection technique. Wackers et al. (1) concluded that significant nonrandom physiologic alterations in ejection fraction should be greater than 10% in normal patients and 5% in abnormal patients. Both analysis techniques are acceptable for detecting ejection fraction changes in this range because the standard error of the estimate was less than 3.1% for both interobserver and intraobserver comparisons (Table 1). Observer 1 changed edge detection variables in 8 of 100 patients for the first automatic detection analysis series and 11 of the same 100 patients for the second series. Therefore, the consistency of measures for the automatic technique also reflects the consistency of Observer 1, who did alter edge detection variables in a small percentage of patients. In the remaining patients, the variation in ejection fraction results for the automatic technique reflects a sensitivity to selection of the left ventricular centroid by the operator. The ability of the method to provide consistent results with low-count images was shown by the near-unity regression line (0.995) and small mean absolute difference (2.6%) between low- and high-count studies in the same patient.

The accuracy of the analysis methods is shown by the excellent comparisons with clinically interpreted ejection fractions (Table 1) as well as the cardiac phantom results. The accuracy is limited by variables that affect all planar gated blood-pool ejection fraction methods, including overlap between the left ventricle and left atrium and accurate determination of background counts. Techniques, such as electrocardiographic gated magnetic resonance studies or SPECT gated blood-pool studies may provide more accurate measures of ejection fraction.

### Clinical Application

The primary advantage of this edge detection technique is that it uses spatially variable edge detection parameters that are shown (Fig. 1) to vary significantly with spatial location. Because the derivative edge detection parameters are based on fourth-order polynomial fits, good edges are determined even with noisy images. Edge detection based on all three parameters (amplitude and first and second derivatives) tends to make edge detection more consistent because it is not dependent on a single parameter. For example, an amplitude threshold method could detect either the left ventricular or right ventricular border at the septum. The addition, however, of a negative count derivative constraint limits the edge to the left ventricular border.

This edge detection technique works well for ventricles of various sizes because all edge parameters are normalized to the maximum value in that image frame. The left ventricle can be very simply modeled as a sphere. The count profile of a sphere would have the shape of a sine wave with amplitude proportional to the diameter. The normalized derivative would be a cosine wave and the second derivative a negative sine wave. Profiles normalized to the diameter for both large and small spheres would have identical edge parameters. This insensitivity to size also promotes accurate edge detection throughout the cardiac cycle because the edge parameters are normalized at

each time point. For left ventricles that have a markedly different shape, as a result of aortic regurgitation or left ventricular hypertrophy, for example, the standard template may not provide well-defined ventricular borders. Such ventricles will require use of the semiautomatic method, which enables the operator to define local edge detection parameters unique to that ventricle.

The automatic technique failed in three patients for Observer 2 because extracardiac structures were detected. Observer 2 did not alter the edge detection parameters. Reducing the parameter that smoothes the first guess at the edge in the first frame from 0.5 to 0.3 resulted in correct edge identification for each patient edge that could not be identified correctly by Observer 2.

### Template Definition

The most important element of the automatic method that affects edge detection is the template of edge detection parameters. The number of patients included in the template, similarity of ventricular anatomy and operator definition of borders will affect the mean parameters included in the template. If an operator desires the border to be smaller or larger for the entire ventricle, this can be accomplished by adjusting the edge detection threshold, which modifies all edge parameters in a linear manner. If observers differ as to ventricular border detection on a regional basis, separate templates can be generated according to each user's preference. For the current template, the edge parameters for the 15 patients included for template generation were compared graphically. On the basis of visual assessment, no patient was identified as significantly different from any other patient. Future template generations could use more sophisticated statistical measures to ensure that no patient included in the template is an outlier. The primary effect of a different template would be to raise or lower all ejection fraction values, with little effect on consistency. Therefore, a different template may change the institutional standard value used for definition of a normal ejection fraction.

A figure of merit for edge detection parameters might be the change in parameter values between adjacent pixel locations divided by the standard deviation of that parameter. Therefore, a parameter that exhibits a large change in value for adjacent pixel locations with a small standard deviation of values is more likely to provide accurate edge detection. A plot of this figure of merit for each spatial location and all edge parameters is shown in Figure 4. These data are based on the 15 patient templates used to generate the template used with the automatic method. This figure of merit could be used as a weighting factor for each parameter when calculating the mean square difference between measured and template edge parameter values. This would make edge detection more sensitive to parameters with a higher figure of merit. Currently, all square differences have a unity weighting factor. Weighting based on figure of merit would result in the first derivative having little effect for edge detection along the lateral wall (Fig. 4). In general, on the basis of this figure of merit, the second derivative is the most significant edge detection parameter.

Optimization of edge parameters throughout the cardiac cycle could be achieved by developing templates for frames at various phases of the cardiac cycle. The left atrium fills, the septum thickens, and the right ventricular counts change during the cardiac cycle, all of which affect edge parameters.
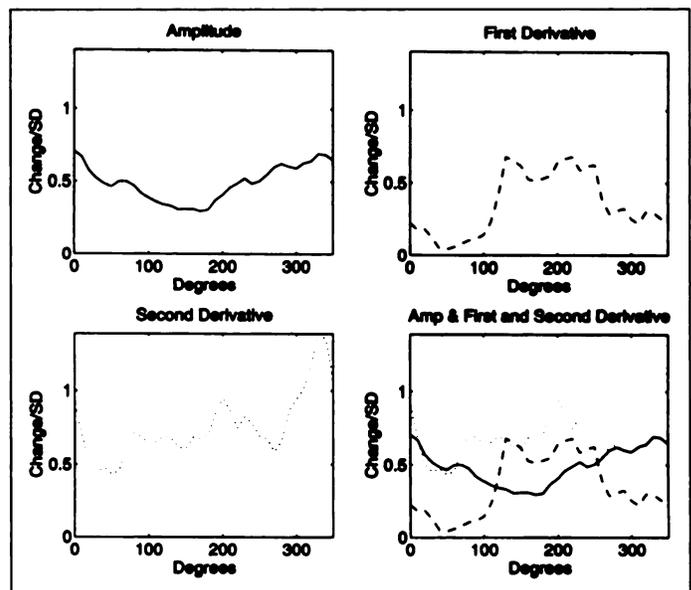


**FIGURE 4.** Edge parameter figure of merit, equal to the change in parameter values with pixel location divided by the standard deviation of the parameter at that point, shown for amplitude (—), first derivative (---) and second derivative (···).

## CONCLUSION

This edge detection methodology could have application in other aspects of nuclear medicine as well as other imaging modalities. To be detected with this radial coordinate system, organs must have a convex geometry. For organs with similar anatomy between patients, such as the kidney, a template of edge parameters could be developed for automatic detection. For organs with varying morphology between patients, such as the stomach and gallbladder, the operator would need to identify these organs in a frame with significant activity. In addition to tracking changes in tracer distribution, this technique may also be capable of tracking edge changes caused by patient motion.

## REFERENCES

1. Wackers FJT, Berger HJ, Johnstone DE, et al. Multiple gated cardiac blood-pool imaging for left ventricular ejection fraction: validation of the technique and assessment of variability. Am J Cardiol 1979;43:1159–1166.
2. Burow RD, Strauss W, Singleton R, et al. Analysis of left ventricular function from multiple gated acquisition cardiac blood-pool imaging. Circulation 1977;56:1024–1028.
3. Bacharach SL, Green MV, Borer JS, Hyde JE, Farkas SP, Johnston GS. Left-ventricular peak ejection rate, filling rate, and ejection fraction-frame rate requirements at rest and exercise: concise communication. J Nucl Med 1979;20:189–193.
4. Green MV, Brody WR, Douglas MA, et al. Ejection fraction by count rate from gated images. J Nucl Med 1978;19:880–883.
5. Okada RD, Kirshenbaum HD, Kushner FG, et al. Observer variance in the qualitative evaluation of left ventricular wall motion and quantitation of left ventricular ejection fraction using rest and exercise multigated blood-pool imaging. Circulation 1980;61:128–136.
6. Reiber JHC. Quantitative analysis of left ventricular function from equilibrium gated blood-pool scintigrams: an overview of computer methods. Eur J Nucl Med 1985;10:97–110.
7. Chang W, Henkin RE, Hale DJ, Hall D. Methods for detection of left ventricular edges. Semin Nucl Med 1980;10:39–52.
8. Hawman EG. Digital boundary detection techniques for the analysis of gated cardiac scintigrams. Optical Eng 1981;20:719–725.
9. King MA, Doherty PW, Schwinger RB, Jacobs DA, Kidder RE, Miller TR. Fast count dependent digital filtering of nuclear medicine images: concise communication. J Nucl Med 1983;24:1039–1045.
10. King MA, Doherty PW, Schwinger RB, Penney BC. Two-dimensional filtering of SPECT images using the Metz and Wiener filters. J Nucl Med 1984;25:1234–1240.